

## Supporting Information

# A magnesium MOF as highly selective fluorescence sensor for CS<sub>2</sub> and nitroaromatic compounds

Zhao-Feng Wu,<sup>a,b</sup> Bin Tan,<sup>a,b</sup> Mei-Ling Feng,<sup>a</sup> An-Jian Lan<sup>a,\*</sup> and Xiao-Ying Huang<sup>a,\*</sup>

<sup>a</sup> State Key Laboratory of Structural Chemistry, Fujian Institute of Research on the Structure of Matter, the Chinese Academy of Sciences, Fuzhou, Fujian 350002, P.R. China.

<sup>b</sup> University of the Chinese Academy of Sciences, Beijing 100049, P.R. China.

Fax: +86 591 83793727; Tel: +86 591 83793727; E-mail: [xyhuang@fjirsm.ac.cn](mailto:xyhuang@fjirsm.ac.cn)

**Table S1.** Selected bond lengths (Å) and angles (°) for compound **1<sup>a</sup>**.

Mg(1)-O(9)	2.0195(15)	Mg(2)-O(9)	2.0859(15)
Mg(1)-O(10)	2.0352(18)	Mg(2)-O(11)	2.1033(17)
Mg(1)-O(1)	2.0400(16)	Mg(2)-O(5)	2.1310(15)
Mg(1)-O(6)#1	2.0543(16)	Mg(2)-Mg(3)	3.1523(7)
Mg(1)-O(7)#2	2.1678(15)	Mg(3)-O(3)#3	2.0501(14)
Mg(1)-O(8)#2	2.2604(15)	Mg(3)-O(3)#5	2.0501(14)
Mg(1)-C(10)#2	2.550(2)	Mg(3)-O(9)	2.0812(13)
Mg(1)-Mg(3)	3.5147(7)	Mg(3)-O(9)#1	2.0812(13)
Mg(1)-Mg(2)	3.5275(10)	Mg(3)-O(5)	2.1302(13)
Mg(2)-O(4)#3	2.0423(16)	Mg(3)-O(5)#1	2.1302(13)
Mg(2)-O(8)#4	2.0617(15)	Mg(3)-Mg(2)#1	3.1523(7)
Mg(2)-O(2)	2.0635(16)	Mg(3)-Mg(1)#1	3.5147(7)
O(9)-Mg(1)-O(10)	113.54(7)	O(2)-Mg(2)-O(11)	89.32(7)
O(9)-Mg(1)-O(1)	97.70(6)	O(9)-Mg(2)-O(11)	170.92(7)
O(10)-Mg(1)-O(1)	86.19(7)	O(4)#3-Mg(2)-O(5)	90.77(6)
O(9)-Mg(1)-O(6)#1	96.60(6)	O(8)#4-Mg(2)-O(5)	83.80(6)
O(10)-Mg(1)-O(6)#1	85.15(8)	O(2)-Mg(2)-O(5)	173.30(7)
O(1)-Mg(1)-O(6)#1	165.33(7)	O(9)-Mg(2)-O(5)	79.63(5)
O(9)-Mg(1)-O(7)#2	151.19(7)	O(11)-Mg(2)-O(5)	95.46(7)
O(10)-Mg(1)-O(7)#2	95.21(7)	O(3)#3-Mg(3)-O(3)#5	180.00(9)
O(1)-Mg(1)-O(7)#2	85.54(6)	O(3)#3-Mg(3)-O(9)	90.46(5)
O(6)#1-Mg(1)-O(7)#2	83.49(6)	O(3)#5-Mg(3)-O(9)	89.54(5)
O(9)-Mg(1)-O(8)#2	92.30(6)	O(3)#3-Mg(3)-O(9)#1	89.54(5)
O(10)-Mg(1)-O(8)#2	154.14(7)	O(3)#5-Mg(3)-O(9)#1	90.46(5)
O(1)-Mg(1)-O(8)#2	89.52(6)	O(9)-Mg(3)-O(9)#1	180.0
O(6)#1-Mg(1)-O(8)#2	93.13(6)	O(3)#3-Mg(3)-O(5)	88.52(6)
O(7)#2-Mg(1)-O(8)#2	59.01(5)	O(3)#5-Mg(3)-O(5)	91.48(6)
O(4)#3-Mg(2)-O(8)#4	170.08(7)	O(9)-Mg(3)-O(5)	79.76(5)
O(4)#3-Mg(2)-O(2)	94.54(7)	O(9)#1-Mg(3)-O(5)	100.24(5)
O(8)#4-Mg(2)-O(2)	91.52(6)	O(3)#3-Mg(3)-O(5)#1	91.48(6)
O(4)#3-Mg(2)-O(9)	90.20(6)	O(3)#5-Mg(3)-O(5)#1	88.52(6)
O(8)#4-Mg(2)-O(9)	96.96(6)	O(9)-Mg(3)-O(5)#1	100.24(5)
O(2)-Mg(2)-O(9)	96.24(6)	O(9)#1-Mg(3)-O(5)#1	79.76(5)
O(4)#3-Mg(2)-O(11)	82.19(7)	O(5)-Mg(3)-O(5)#1	180.0

O(8)#4-Mg(2)-O(11) 90.04(7)

Symmetry transformations used to generate equivalent atoms: #1 -x+1,-y,-z+1; #2 x-1, y, z+1; #3 x+1, y, z; #4 -x+1,-y,-z; #5 -x,-y,-z+1; #6 x-1,y,z; #7 x+1, y, z-1; #8 -x-1,-y+1,-z+1; #9 -x,-y+1,-z+2.

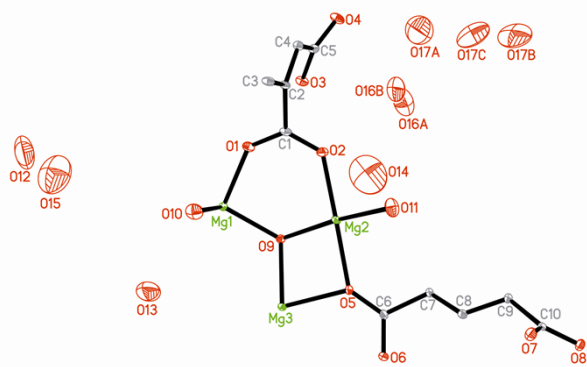


Fig. S1 ORTEP of the asymmetric unit of **1** (30% probability level).

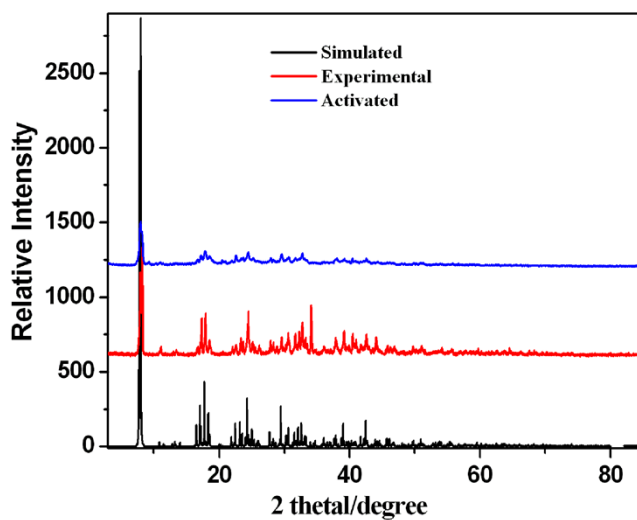


Fig. S2 The PXRD pattern of compound **1** is comparable to the simulated from the single crystal X-ray data and after activated at 100°C for 5h, respectively.

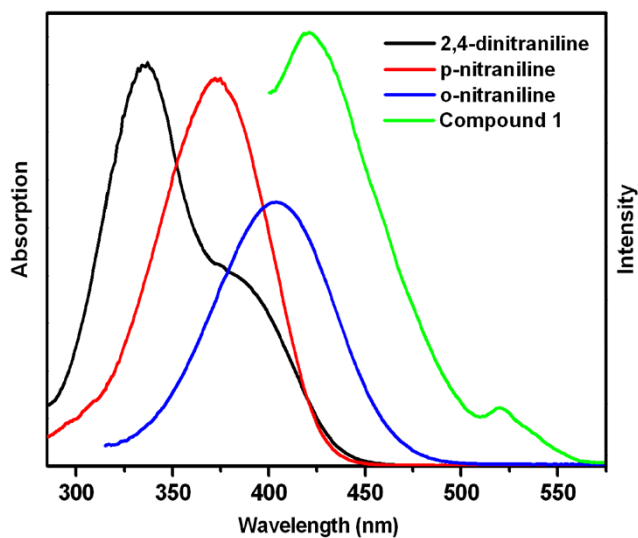


Fig. S3 PL emission spectrum of **1** and absorption spectra of 2,4-dinitraniline, O- and p-nitraniline in  $\text{CH}_3\text{CH}_2\text{OH}$  ( $1 \times 10^{-5}$  M).

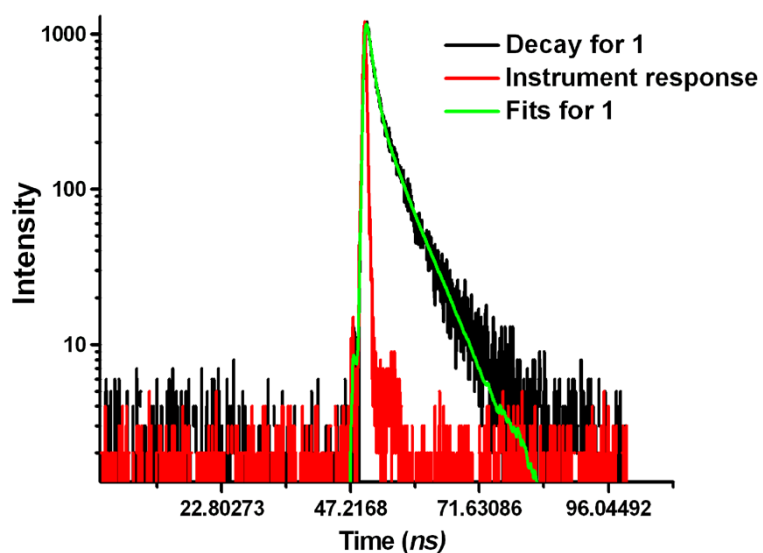


Fig. S4 The decay curve of compound 1.

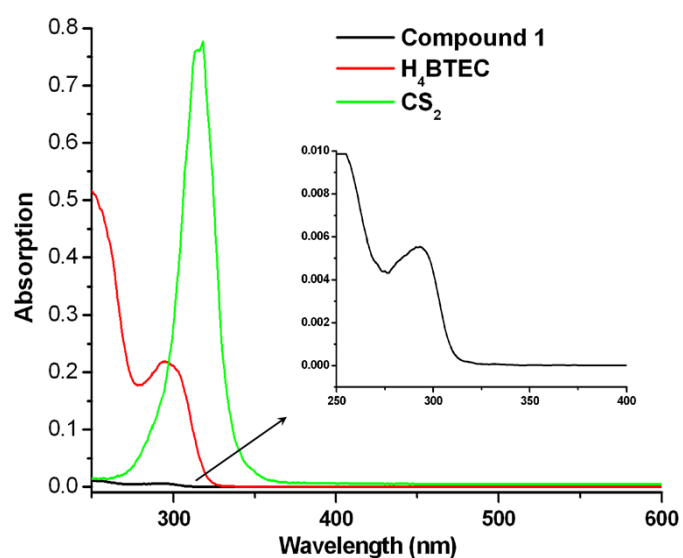


Fig. S5 Absorption spectra of compound 1, H<sub>4</sub>BTEC ligand and CS<sub>2</sub> in CH<sub>3</sub>CH<sub>2</sub>OH ( $1 \times 10^{-5}$  M).

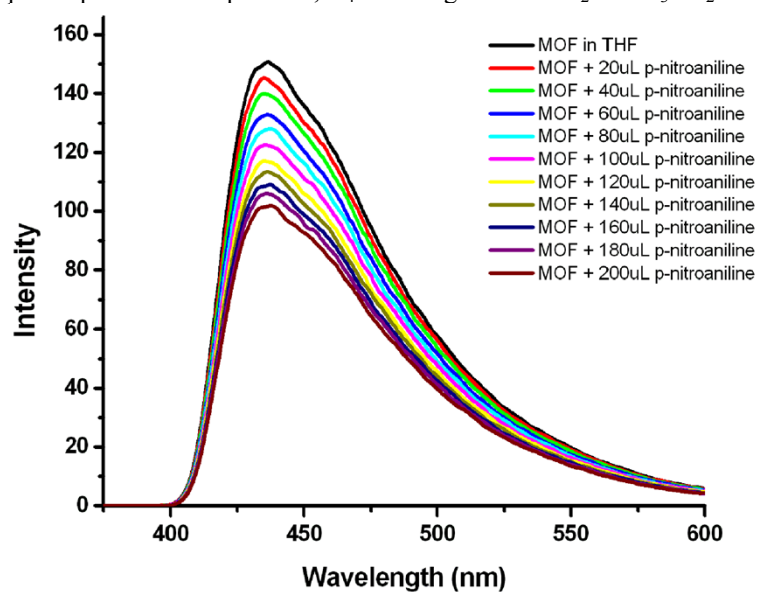


Fig. S6 PL spectra of compound 1 dispersed in THF by gradual addition of  $10^{-3}$  M solution of p-nitraniline in ethanol.

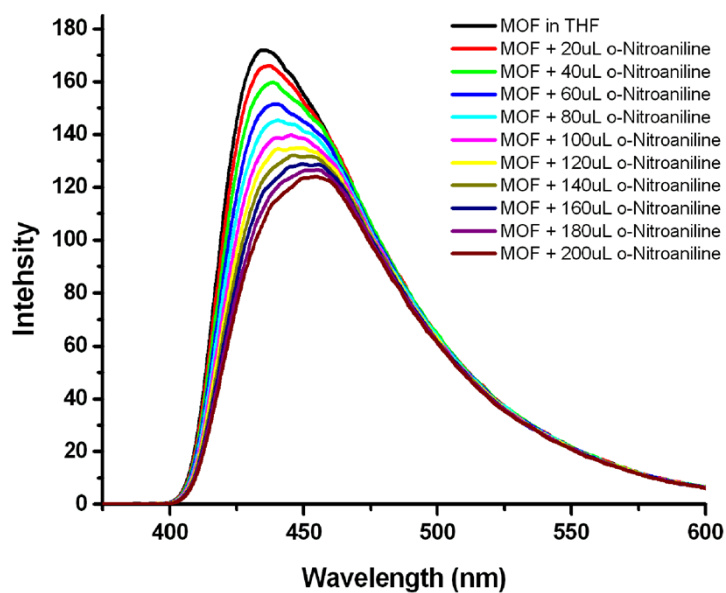


Fig. S7 PL spectra of compound **1** dispersed in THF by gradual addition of  $10^{-3}$  M solution of o-nitraniline in ethanol.

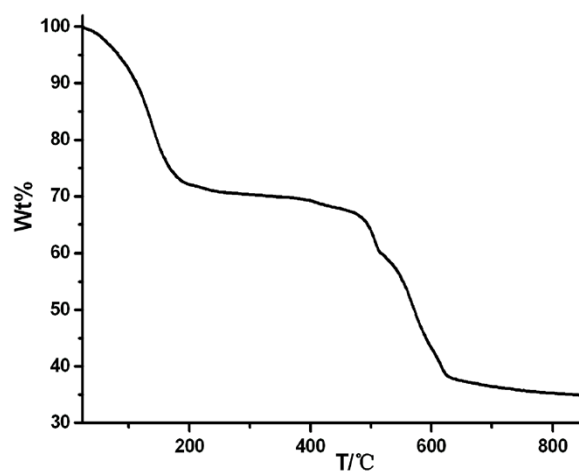


Fig. S8 TGA curves of compound **1**.

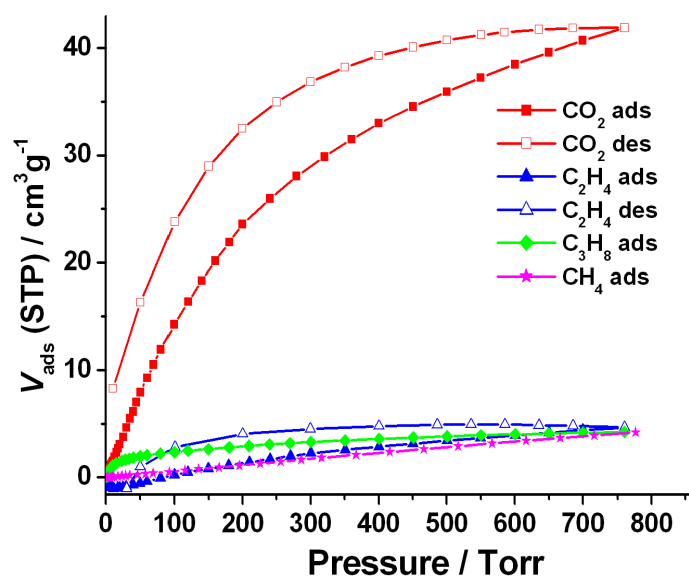


Fig. S9 The  $\text{CO}_2$ ,  $\text{CH}_4$ ,  $\text{C}_2\text{H}_4$  and  $\text{C}_3\text{H}_8$  adsorption isotherms of **1'** at room temperature.

## Gas adsorption

As a good candidate for gas storage, the Mg-MOFs could provide a boost in reaching the mass percentage (wt%) of gas storage targets because of the lower density compared to the MOFs based on transition-metals.<sup>1</sup> Hence we investigated the gas adsorption behaviour of compound **1**. In the TG curve of **1** (Fig. S8), the first weight loss of 28.5% at about 220 °C corresponds to the loss of guest water molecules (calcd: 28.5%, corresponding to the solvent water molecules) and the BTEC ligand decomposes after 500 °C. In order to remove the guest water molecules, compound **1** was activated at 100 °C under vacuum. The activated one (**1'**) has a high degree of crystallinity evidenced by the PXRD characterization (Fig. S2), which indicates the rigid framework of compound **1** still maintained. Gas adsorption measurements show that the CO<sub>2</sub> adsorption of **1'** exhibits the adsorption of 41.9 cm<sup>3</sup>·g<sup>-1</sup> at 298.15 K and 1 atm (Fig. S9). In the same measurement conditions, while for other energy gases such as CH<sub>4</sub>, C<sub>2</sub>H<sub>4</sub> and C<sub>3</sub>H<sub>8</sub>, **1'** shows almost no adsorption behaviour. Compared to the former reported Mg-MOFs for CO<sub>2</sub> adsorption at lower 77K or 87K,<sup>2</sup> **1'** could selectively separate CO<sub>2</sub> from the energy gases at room temperature which may have the purification effects.

## references

1 (a) D. Britt, H. Furukawa, B. Wang, T. G. Glover and O. M. Yaghi, *PNAS*, 2009, **106**, 20637; (b) M. Dinca and J. R. Long, *J. Am. Chem. Soc.*, 2005, 127, 9376; c) Y. P. He, Y. X. Tan and J. Zhang, *Cryst. Growth Des.* 2013, 13, 6.

2 Y. E. Cheon, J. Park and M. P. Suh, *Chem. Commun.* 2009, 5436.